Polarity consistent geophone rotation analysis by inversion: Penn West 3D VSP

Robert J. Ferguson

ABSTRACT

The Rig-source VSP/ Offset VSP/ Walkaway VSP of Penn West Petroleum Ltd is used to demonstrate a new geophone rotation analysis. This survey employs non-gimballed geophones in a deviated well-bore and so the orientation of all three components is required for proper wavefield separation. Three walkaway VSP source lines are recorded in a total of 45 geophone levels downhole. Data are gathered according to common receiver and first break energy is analyzed based on the new method. So that absolute measurements can be made for each receiver level, each three component recording is rotated such that all sources for a common receiver reside vertically above that receiver and then first-break analysis is used to point one of the geophone components at the source location. Within each common receiver gather very good agreement is found between sources for the dip between the geophone component and the source location and that good agreement is found for the azimuth of the two remaining components.

INTRODUCTION

A P-wave source is recorded on all three geophone components (3C) similarly S-waves (Toksöz and Stewart, 1984), and so 3-component VSP must be *rotated* into it's three orthogonal components P, H1 and H2. Ferguson (2009) presents an automatic method where, for a non-gimballed geophone in a deviated well, geophone dip ϕ and azimuth θ are determined by inversion and then data rotation is accomplished by matrix multiplication. Maximization of the energy on the desired component points that component at the source, and this is the assumption central to common rotation methods DiSiena et al. (1984) as well as in Ferguson (2009); P-wave first arrivals (or S-wave first arrivals) are identified on the 3C recording, then amplitudes extracted within a window around the first arrivals. As an extra constraint, Ferguson (2009) extends maximization to include normalize the 3C recording so that the desired waveform (pure P-wave on the Z component for example) and the corresponding 3C component (the Z recording) have equal polarity.

The result is an inversion-based method by which a 3×3 Euler rotation matrix is deduced from 3C data. This matrix can be used to rotate the 3C data so that on component (the principle P-wave component) points at the P-wave source and the H1 and H2 components are rotated such that H1 is contained within the vertical plane through the source / receiver direction.

THEORY

The essential equations from Ferguson (2009) relate the *ideal* 3C recording W (a $3 \times N$ data matrix for N time samples) to the actual recording V $(3 \times N)$ through unitary rotation operators G_θ and G_ψ where ψ and θ are *dip* and *azimuth* respectively of the geophone; Angles ψ and θ are measured relative to a coordinate system defined by the plane that

contains the Z component (the vertical component) and one of H_1 and H_2 (the horizontal components); The plane will be orthogonal to the other H component.

Operators G_θ and G_ϕ are applied in series and their combination

$$G_{\theta\,\phi} = G_\theta\, G_\phi = \begin{bmatrix} \cos\theta & \sin\theta\,\cos\phi & \sin\theta\,\sin\phi \\ -\sin\theta & \cos\theta\,\cos\phi & \cos\theta\,\sin\phi \\ 0 & -\sin\phi & \cos\phi \end{bmatrix}, \tag{1}$$

converts W into V according to

$$V = G_{\theta\,\phi}\, W. \tag{2}$$

Operator $G_{\theta,\phi}$ can be thought of as a Euler matrix that applies a *roll*, *pitch*, and *yaw* rotation in a right-handed coordinate system (Weisstein, 2012). Here, however, geophone orientation is specified completely by pitch (about the z-axis) and roll (about the x-axis). Equation 2 is solved for $G_{\theta,\phi}$ by inversion with the condition that the polarity of the preferred component (one of Z, H_1, or H_2) is the same on V and W (Ferguson, 2009). Correction of the recorded data V is done simply through finding the inverse

$$F_{\theta,\phi} = G^{-1}_{\theta\,\phi} = G^T_{\theta\,\phi}, \tag{3}$$

where T indicates the matrix transpose and, according to equation 1, $G_{\theta,\phi}$ is unitary Ferguson (2009). With $F_{\theta,\phi}$ calculated, then, the solution for the desired signal W is simply a matrix multiplication according to

$$W = F_{\theta,\phi}\, V. \tag{4}$$

REAL DATA EXAMPLE

Data from the *Penn West 102 PEM 10-11-48-9* Rig-source VSP/ Offset VSP/ Walkaway VSP are obtained for this study. The data were acquired on March 29, 2007 and consist of a zero-offset vertical seismic profile (VSP), a far offset VSP, and a 3D VSP that consists of four walkaway lines (Daniels, 2009). For the proposes of this study only the latter data are considered, and of these, orthogonal lines 1 and 2 plus diagonal line 6 are considered.

Acquisition

As is shown in Figure 1(a), the well associated with the survey is deviated with an average well dip of ~ 15 degrees from vertical (Figure 1(b)) and ~ 40 degrees azimuth to the south-east (Figure 1(c)). The geophones are non-gimballed so that the Z component does not necessarily line up with the direction of gravity.

Three distinct tool levels were used where the 16-level tool was moved three times during acquisition for a total of 48 receiver levels. Geophone 15 of the 16 in the tool is found to be dead however, so the actual number of live levels is 45. The 3D VSP geometry is given in Figure 2, and a legend for the symbols in this figure is given in Table 1. The "shallow" tool levels correspond to the furthest offsets on Figure 2, the "intermediate" levels to intermediate offsets, and the "deep" levels correspond to the nearest offsets.

Pre-processing

Data orientation by the Ferguson (2009) process requires a window about the first arrivals of interest (in this case primary P-waves). The centre of this window is aligned with the picks of the first arrivals that are found to be well determined using the *short-term-average / long-term-average* (STA / LTA) method of Oye and Roth (2003). The lengths of the short and long windows for STA / LTA are determined by trial and error; window length is determined by how well the first-breaks flatten when the first-break picks are applied as statics.

Data for lines 1, 2, and 6 are shown in Figures 3, 4, and 5, and they are ordered in common-shot configuration within each line. First breaks are annotated on panel (a) of these Figures, and the corresponding flattened data are shown in panel (b) of these Figures. With very little exception, the first breaks are found to flatten for short and long window lengths of 11 and 21 points respectively (Table 2).

Reconcile geometry

From the perspective of the common receiver, direct comparison can be made of all θ and ϕ estimates if the geometries of the associated shots are reconciled into a uniform source / receiver orientation. The optimal way to do this is to ray-trace between each source / receiver pair using the exact velocity model so that the incident dips and azimuths are known and then used to compensate (rectify / reconcile) θ and ϕ estimates for each pair - the optimal result would be identical values of θ and ϕ for each pair regardless of the source location.

Here, for simplicity, the assumption of straight rays is made and reconciliation proceeds as follows. For a source W located at the origin of a coordinate system the recording V that corresponds to the geophone orientation θ, ϕ is determined by equation 2. A source located at x, y, z in the coordinate system introduces another unitary operator G_{xyz} according to

$$V = G_{xyz}\, G_{\theta\,\phi}\, W, \tag{5}$$

where $G_{\theta\,\phi}$ is the unitary operator from equation 2 that applies the θ and ϕ rotations simultaneously. Unitary operator G_{xyz} rotates the source location from the origin of the absolute coordinate system to position x, y, z. For a source at x, y, z the recording V at the geophone will be the result of the source wavefield W with two rotation operators applied - $G_{\theta\,\phi}$ due to the orientation of the geophone and G_{xyz} due to the orientation of the source. From equation 3, correction operator $F_{\theta,\phi}$ is determined through the solution of

$$G_{xyz}^{T}\, V = G_{\theta\,\phi}\, W, \tag{6}$$

for $G_{\theta\,\phi}$ where G_{xyz} is applied as an inversion operator to the 3C recording V prior to inversion for $G_{\theta,\phi}$.

Rotation analysis

An "intermediate" depth geophone (1144 m) is analyzed here as a demonstration. Source locations for lines 1, 2, and 6 are plotted in plan view in Figure 6, and the re-

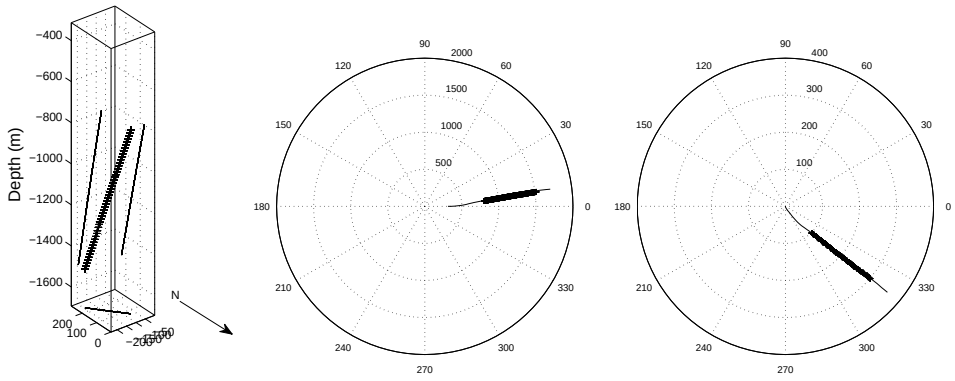

(a) (b) (c)

FIG. 1. Deviated well trajectory. a) The black, crosses indicate the trajectory of the well. Solid lines indicate the vertical and horizontal projections of the well. b) Polar plot of well trajectory dip verses radial distance - average dip is $\sim$ 15 degrees from vertical. The tool locations are plotted as "+". c) Polar plot of well trajectory azimuth verses radial distance - average azimuth is $\sim$ 40 degrees to the southeast.

Description	Depth (mKB)	Source symbol on Figure 2
Shallow	798 - 1025	"+"
Intermediate	1038 - 1265	"$\diamond$"
Deep	1278 - 1505	"$\bullet$"

Table 1. Source symbols and tool depths below Kelly Bushing (KB) for the VSP.

ceiver is just to the left of the origin. Each source contributes an estimate of θ and ϕ for the receiver and these are plotted in Figures 7 and 8 respectively. For this receiver, the average θ estimate is about 40 degrees but the associated errors are quite large. The average ϕ is about 60 degrees and error here is less than that for θ. Estimates of θ and ϕ for the entire 3D VSP are shown in Figure 9. Dip ϕ increases with depth from about 55 degrees to about 70 degrees and this appears to be inconsistent with the 15 degree well trajectory - for non-gimballed geophones, ϕ estimates should be about 15 degrees. It is noted here that for every receiver, ϕ estimates are usually quite consistent source-to-source so there is probably a problem with the chosen coordinate frame, but it is found to have no obvious relationship. Azimuth θ decreases with depth from about 70 degrees to about 10 degrees. Overall, θ agreement source-to-source is not as good as for ϕ.

Process	Parameters
Assign geometry	Shot ordered
First break picks	STA / LTA $\alpha = 11$ and $\beta = 21$

Table 2. VSP pre-processing flow. For STA / LTA above α and β refer to the numbers of points in the short (S) and long (L) moving average.

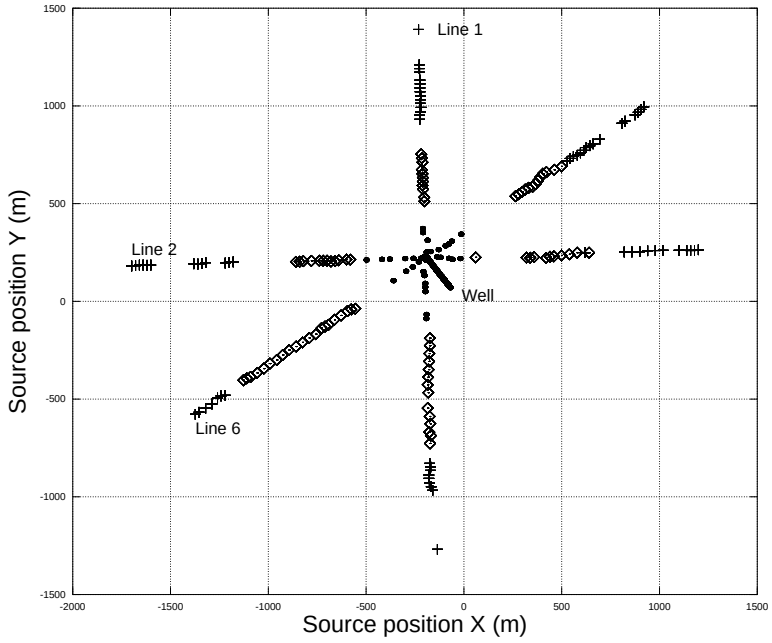

FIG. 2. Source locations plus the well trajectory for the Pen West 102 3D lines 1, 2, and 6. The "+" symbol indicates source data acquired for the "shallow" tool level (Table 1), ◇ for the "intermediate" level, and · for the "deep" level. The well trajectory is deepest a the intersection of the lines, and becomes shallower to the SE.

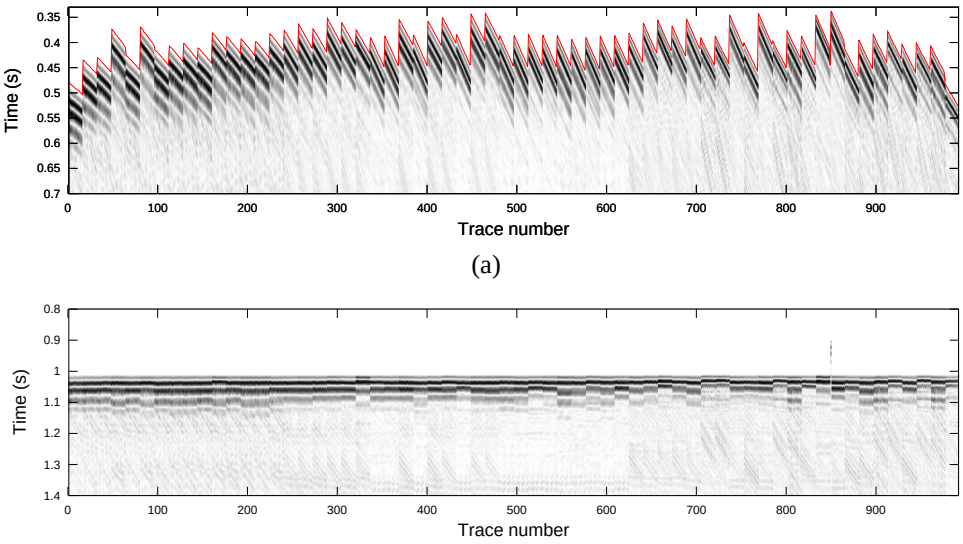

FIG. 3. Penn West 102 3D ay/grey/gc line 1. a) The data are plotted as grey scale and first break picks are plotted as a solid line. b) First breaks are used to align traces as a check on pick quality.

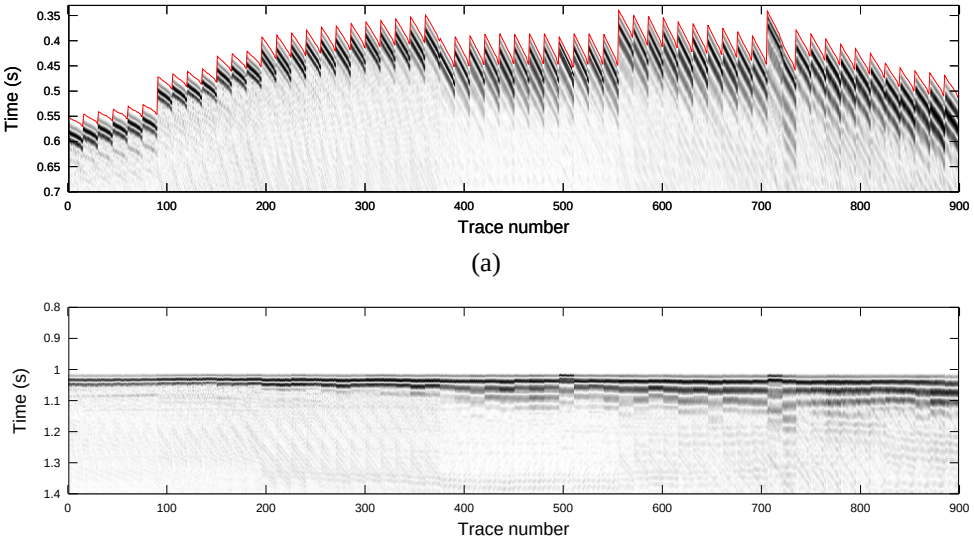

FIG. 4. Penn West 102 3D VSP line 2. a) The data are plotted as grey scale and first break picks are plotted as a solid line. b) First breaks are used to align traces as a check on pick quality.

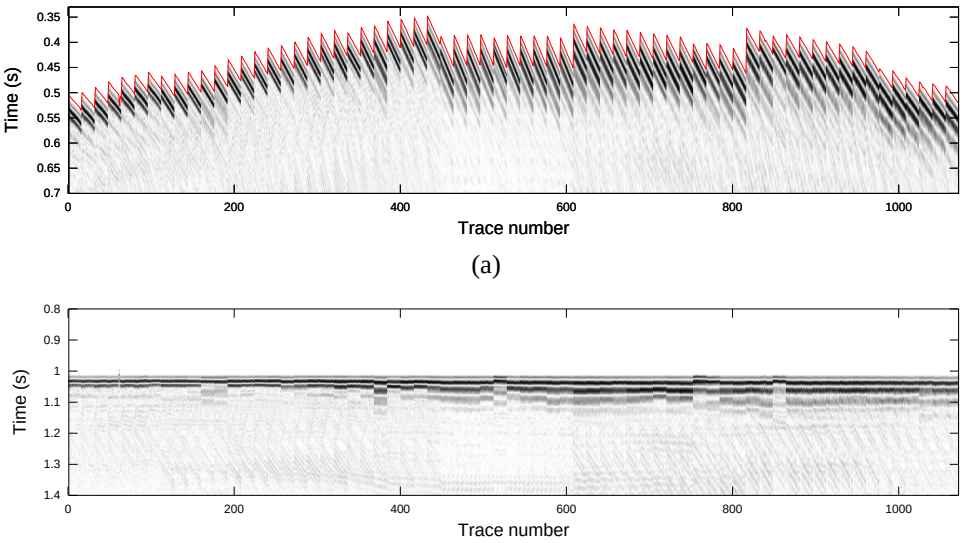

FIG. 5. Penn West 102 3D VSP line 6. a) The data are plotted as grey scale and first break picks are plotted as a solid line. b) First breaks are used to align traces as a check on pick quality.

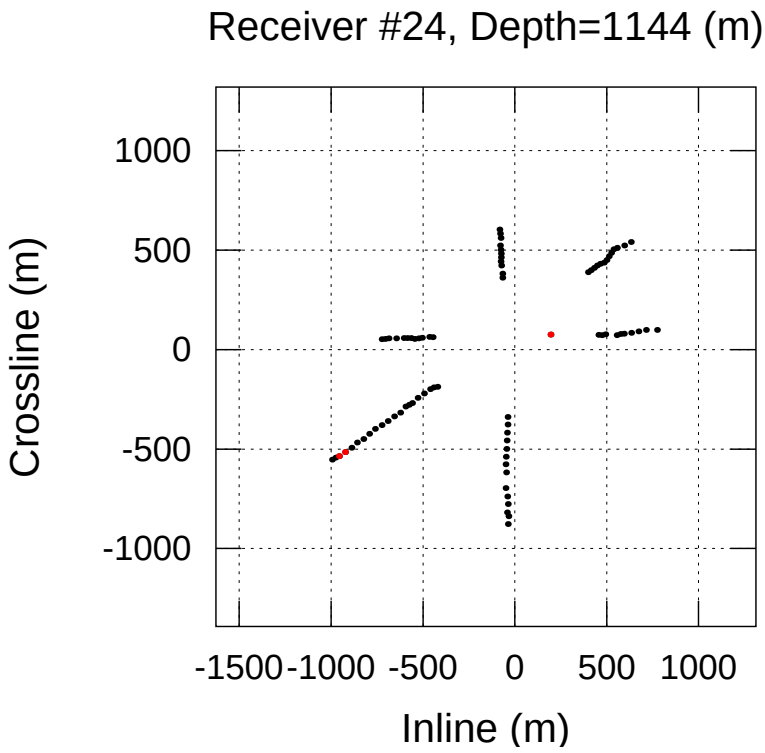

FIG. 6. Plan view of sources for receiver 24 (depth = 1144 m). Source positions for lines 1, 2 and 6 radiate out from the origin and the lone dot indicates the receiver location.

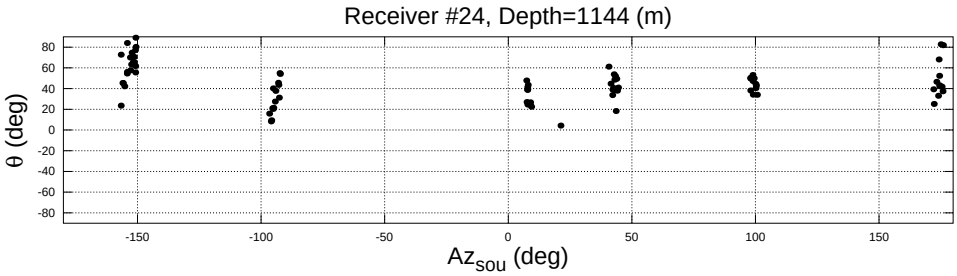

FIG. 7. Geophone azimuth estimate verses source-receiver azimuth for the CRP in Figure 6.

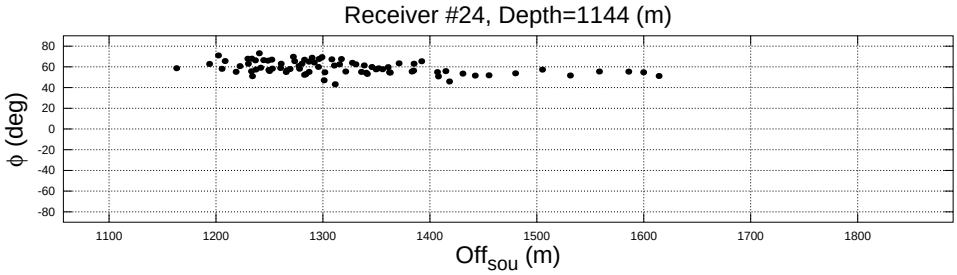

FIG. 8. Geophone dip estimate verses source-receiver offset for the CRP in Figure 6.

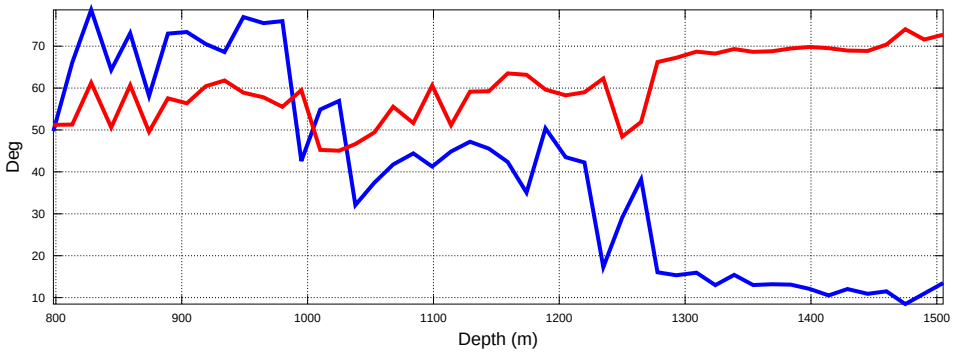

FIG. 9. Averaged estimates of θ (blue line) and ϕ (red line) for all depths.

CONCLUSIONS

Application of this method shows great promise in synthetic tests and this is demonstrated in previous work by the author. The method has the advantage that it proceeds automatically without user intervention and it returns estimates of the dip ϕ and azimuthθ that describe the orientation of each geophone. For the real data example presented here, however, a number of problems are illuminated: 1) though good agreement source-to-source (within a common receiver) is achieved, the estimated ϕ values are not in close agreement with the value of 15 degrees expected for a non-gimballed geophone in this 15 degree wellbore. 2) Large error is associated with θ estimates source-to-source indicate that there is an outstanding issue that is yet unresolved. Data are relatively noise free so the θ errors are expected to be the result of systematic error rather than measurement error. The data are analyzed here in a nearly unprocessed form so a more careful processing procedure that will achieve true relative amplitude will be pursued.

ACKNOWLEDGEMENTS

I wish to thank Kristopher Innanen of CREWES for his helpful discussion, and I wish to thank also the sponsors, faculty, and staff of CREWES, and the Natural Sciences and Engineering Research Council of Canada (NSERC, CRDPJ 379744-08), for their support of this work.

REFERENCES

Daniels, S., 2009, Penn west 102 pem 10-11-48-9: Schlumberger data processing report.

DiSiena, J. P., Gaiser, J. E., and Corrigan, D., 1984, Horizontal components and shear wave analysis of three-component VSP data, *in* Toksöz, M. N., and Stewart, R. R., Eds., Vertical seismic profiling, Part B: Advanced concepts, Geophysical Press.

Ferguson, R. J., 2009, Geophone rotation analysis by polarity inversion: CREWES Research Report, **21**.

Oye, V., and Roth, M., 2003, Automated seismic event location for hydrocarbon reservoirs: Computers & Geosciences, **29**, No. 7, 851–863.
URL `http://dx.doi.org/10.1016/S0098-3004(03)00088-8`

Toksöz, M. N., and Stewart, R. R., Eds., 1984, Vertical seismic profiling: Geophysical Press.

Weisstein, E., 2012, Rotation matrix.
URL http://mathworld.wolfram.com/RotationMatrix.html